Electronic Structures and Gas-Phase Reactivities of Cationic Late-Transition-Metal Oxides

Andreas Fiedler,† Detlef Schröder,† Sason Shaik,*,‡ and Helmut Schwarz*,†

Contribution from the Institut für Organische Chemie der Technischen Universität Berlin, Strasse des 17. Juni 135, D-10623 Berlin, Germany, and the Department of Organic Chemistry and the Fritz Haber Center of Molecular Dynamics, Hebrew University of Jerusalem, 91904 Jerusalem, Israel

Received March 7, 1994®

Abstract: The structures, relative stabilities, and multiplicities of the cationic, late-transition-metal oxides FeO^+, CoO^+, NiO^+, and CuO^+ are rationalized on the basis of ab initio computations. The bonding situation in these cations is analogous to that in the dioxygen molecule with a biradicaloid π-bonding, and hence the electronic ground states of these metal oxide cations correspond to their high-spin variants, FeO^+ ($^6\Sigma^+$), CoO^+ ($^5\Delta$), NiO^+ ($^4\Sigma^-$), CuO^+ ($^3\Sigma^-$). Density functional theory augmented with CASPT2D computations is used to explore the reaction surface of $FeO^+ + H_2$ and to unravel the roots of the extremely low reactivity observed for this system. According to these calculations, the reaction violates spin-conservation rules and involves a curve crossing from the sextet ground state to the excited quartet surface, giving rise to a multicentered, energetically low-lying transition structure, from which the hydrido iron hydroxide cation $H-Fe-OH^+$ is formed as the initial oxidation product. The implications of these results with respect to other ion/molecule processes of metal oxide cations with oxidizable organic substrates are discussed.

Introduction

Qualitative concepts are needed to guide the generation and solution of chemical problems. Indeed, such concepts have had a vital role in the development of our understanding of structure and reactivity in organic chemistry.[1] The task is much more challenging though in the chemistry of transition-metal-containing systems.[2] In fact, for small transition-metal fragments even the prediction and assignment of the electronic configuration in the ground states as well as the description of the bonding situations may often be difficult. Moreover, the degeneracy of various energetically low-lying excited states which may contribute to the reactivity of transition-metal fragments complicates the picture in comparison with a single-state potential energy surface, as often encountered in organic reactions. In addition, the situation may further be complicated by spin−orbit coupling mediated changes of the multiplicities of the various intermediates *en route* to the products of an organometallic reaction. Hence, there is a need to develop simple concepts which may assist the experimental research to pattern the existing data and to articulate new problems. The goal of the present paper is to use FeO^+ as an example in order to develop the requisite insight for the reactivity manifold of the late-first-row transition-metal oxide cations, (FeO^+, CoO^+, NiO^+, and CuO^+) with molecular hydrogen and hydrocarbons.

Let us first illustrate the problem and its complexity. C−H and C−C bond activations of hydrocarbons by metal oxides are of fundamental interest in organic chemistry, biochemisry, and catalyst research.[3] Gas-phase experiments permit the examination of intrinsic reactivities of metal−oxo species toward oxidizable organic substrates.[4] Such studies allow not only the determination of thermodynamic properties of metal oxides but also the elaboration of kinetic and energetic parameters which influence reaction mechanisms, selectivities, and regiochemistry. Within the last decade the gas-phase reactions of FeO^+ with dihydrogen and a variety of organic molecules have been studied in detail (Scheme 1).[5−10] The elementary steps of these reactions can be classified as follows: In the reaction of FeO^+ with dihydrogen the products are formed via an insertion process (**I**) since other mechanisms, e.g. a hydrogen atom transfer ($\mathbf{H^{\bullet}_T}$), are not energetically feasible.[5,11] The insertion reaction was found to be inefficient and occurs only once in ca. 100 collisions.

† Institut für Organische Chemie der Technischen Universität Berlin.
‡ Hebrew University of Jerusalem.
® Abstract published in *Advance ACS Abstracts,* October 15, 1994.

(1) For examples: (a) Hückel, E. *Z. Phys.* **1931**, *70*, 204. (b) Woodward, R. B.; Hoffmann, R. *The Conservation of Orbital Symmetry*; Academic Press: New York, 1970. (c) Fukui, K. *Theory of Orientation and Stereoselection*; Wiley-Interscience: New York, 1976. (d) Shaik, S. In *New Concepts for Understanding Organic Reactions*; Bertran, J., Csizmadia, I. G., Eds.; Kluwer Academic: Dordrecht, 1989; NATO ASI Series Vol. C267, p 165.

(2) (a) Hoffmann, R. *Angew. Chem., Int. Ed. Engl.* **1982**, *21*, 711. (b) Carter, E. A.; Goddard, W. A., III *J. Phys. Chem.* **1988**, *92*, 5679. (c) Ohanessian, G.; Goddard, W. A., III *Acc. Chem. Res.* **1990**, *23*, 386. (d) Koga, N.; Morokuma, K. *Chem. Rev.* **1991**, *91*, 823.

(3) (a) Hill, C. L., Ed. *Activation and Functionalization of Alkanes*; Wiley: New York, 1989. (b) Davies, J. A.; Watson, P. L.; Liebman, J. F.; Greenberg, A., Eds. *Selective Hydrocarbon Activation*; VCH Publishers, New York, 1990.

(4) For a recent review of gas-phase metal ion chemistry, see: Eller, K.; Schwarz, H. *Chem. Rev.* **1991**, *91*, 1121.

(5) Schröder, D.; Fiedler, A.; Ryan, M. F.; Schwarz, H. *J. Phys. Chem.* **1994**, *98*, 68.

(6) (a) Schröder, D.; Schwarz, H. *Angew. Chem., Int. Ed. Engl.* **1990**, *29*, 1433. (b) Schröder, D.; Fiedler, A.; Hrusák, J.; Schwarz, H. *J. Am. Chem. Soc.* **1992**, *114*, 1215.

(7) (a) Kappes, M. M.; Staley, R. H. *J. Phys. Chem.* **1981**, *85*, 942. (b) Jackson, T. C.; Jacobson, D. B.; Freiser, B. S. *J. Am. Chem. Soc.* **1984**, *106*, 1252. (c) Schröder, D.; Eller, K.; Schwarz, H. *Helv. Chim. Acta* **1990**, *73*, 380. (d) Schröder, D. Ph.D. Thesis, Technische Universtät Berlin D83, 1993.

(8) (a) Buckner, S. W.; Freiser, B. S. *J. Am. Chem. Soc.* **1988**, *110*, 6606. (b) Schröder, D.; Schwarz, H. *Angew. Chem., Int. Ed. Engl.* **1990**, *29*, 1431. (c) Fiedler, A. Diploma Thesis, Technische Universität Berlin, 1992. (d) See also: Loh, S. K.; Fisher, E. R.; Lian, L.; Schultz, R. H.; Armentrout, P. B. *J. Phys. Chem.* **1989**, *93*, 3159.

(9) (a) Schröder, D.; Schwarz, H. *Helv. Chim. Acta* **1992**, *75*, 1281. (b) Becker, H.; Schröder, D.; Zummack, W.; Schwarz, H. *J. Am. Chem. Soc.* **1994**, *116*, 1096.

(10) Schröder, D.; Florencio, H.; Zummack, W.; Schwarz, H. *Helv. Chim. Acta* **1992**, *75*, 1792.

(11) If not mentioned otherwise all thermochemical data were taken from: Lias, S. G.; Bartmess, J. E.; Liebman, J. F.; Holmes, J. L.; Levin, R. D.; Mallard, W. G. *J. Phys. Chem. Ref. Data* **1988**, *17*, Suppl. 1.

0002-7863/94/1516-10734$04.50/0

Scheme 1

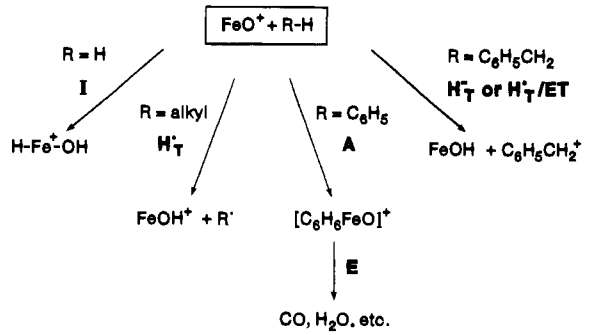

In contrast, the reactions of FeO^+ with alkanes are quite efficient,[6,7] and many of the reactions appear to commence with an initial hydrogen atom transfer ($\mathbf{H^{\bullet}_T}$) from the alkane to the FeO^+ moiety. A third type of mechanism, which is best described as an addition−elimination process (**AE**), seems to be operative in the reactions of FeO^+ with unsaturated hydrocarbons, i.e. ethene[8] and benzene,[9] in which FeO^+ adds to the neutral molecule by an electrophilic attack at a carbon atom, most likely to form a σ-bonded intermediate, and then eliminates the products; alternatively, these reactions may occur via some type of cycloaddition processes. Yet another reaction is exhibited by toluene which undergoes a formal hydride transfer ($\mathbf{H^-_T}$) to FeO^+ to yield a benzyl cation as ionic product.[10] Although electron transfer (**ET**) from toluene to FeO^+ is energetically feasible (the ionization energies of FeO and toluene are comparable within the experimental accuracy)[11] it is not observed with significant efficiency (<0.7%) However, a mechanism involving initial **ET** and subsequent $\mathbf{H^{\bullet}_T}$ (or the reversed sequence) cannot be ruled out.

In most of these examples other mechanisms are also conceivable, and this fact only emphasizes the mechanistic richness of gas-phase oxidation processes. The focus of this paper is to provide an understanding of the possible mechanistic scenarios and to trace the predicted reactivity to electronic structures of the states of FeO^+ and its analogues CoO^+, NiO^+, and CuO^+ as well.[12−14] The problem will be tackled combining high-level computational studies with mnemonic descriptions of the bonding features and the reactivities of the cationic metal oxides.

Computational Details

Ab initio calculations were performed by using the approximate density functional theory (DFT)[15] and the complete active space second-order perturbational theory (CASPT2D).[16] A similar approach was recently used for the description of the cationic $[Fe,O_2]^+$ system.[17] For the DFT calculations we applied the local density functional of Vosko, Wilk, and Nusair,[18] the nonlocal gradient corrections for the exchange part as proposed by Becke,[19] and Perdew's nonlocal gradient corrections for correlation;[20] this will henceforth be referred to as NLSD.

The geometries and energetics of the diatomic metal oxide cations (MO^+: M = Fe, Co, Ni, and Cu) were computed by using the linear combination of Slater-type orbitals (STO) approach which permits the unambiguous assignment of the electronic configurations of MO^+; these NLSD computations were performed with the ADF program package (Version 2.01).[21] The valence electrons were described by double-ζ STO basis sets (4s,3d,4p on the metal and 2s,2p on the oxygen atom, respectively), and the inner electrons were treated by the frozen core approximation. For the mnemonic description of the metal oxide cations in terms of molecular orbital theory, the wave functions and their associated molecular orbitals were computed at the CAS level by using the GAMESS program package.[22]

Explorations of the quartet and sextet potential energy surfaces for the reaction of FeO^+ with molecular hydrogen were performed by using the DGAUSS program package (Version 2.0)[23] and by employing the linear combination of Gaussian-type orbitals (GTO) approach at the NLSD level of theory. The all-electron GTO basis sets of the atoms had double-ζ valence polarization qualities. All stationary points were characterized as minima or first-order transition structures by evaluating the frequencies and normal modes by using analytical first derivatives and a finite difference scheme for the force−constant matrix. The harmonic frequencies of the species are available from the authors upon request. Subsequently, the energies of the relevant species **1**, **2**, and **3** (Scheme 4) for the low-lying roots in all spatial and both spin symmetries were calculated at the CASPT2D level of theory by using large atomic natural orbital (ANO) basis sets: (8s4p3d)/[3s2p1d] for hydrogen,[24] (14s9p4d3f)/[5s4p3d2f] for oxygen,[24] and (21s15p10d6f4g)/[8s7p6d4f2g] for the iron atom.[25] The active MO space in the CAS calculations was derived from the 1s orbitals of the hydrogen atoms, the 2s and 2p orbitals on oxygen, and the 4s and 3d orbitals of iron. All electrons were correlated in the perturbational treatment. These CAS calculations were performed in C_s symmetry with the MOLCAS-2 program package.[26] All computations were performed on either IBM/RS 6000 workstations or a CRAY-YMP computer.

Results and Discussion

A. Electronic Structures of MO^+. Table 1 contains the bond lengths and relative stabilities of the various lowest-lying states for FeO^+, CoO^+, NiO^+, and CuO^+. On the NLSD level of theory the ordering for the sextet and quartet states of FeO^+ and the spacing of the states are in reasonable agreement with more sophisticated calculations at the CASPT2D level of theory.[12] For example, the separation of the $^6\Sigma^+$ and $^4\Phi$ states of FeO^+ is calculated as 1.1 eV by using NLSD and as 0.8 eV by the CASPT2D approach: This difference is within the computational error of both methods and will not affect our general conclusions with respect to the high-spin ground states of the metal oxide cations. Furthermore, our NLSD results for FeO^+ are also in accord with the predictions of Carter and Goddard.[13]

For CoO^+ and NiO^+ our results disagree with the Carter−Goddard[13] assignment of a $^3\Sigma^-$ ground state for CoO^+ and a $^2\Pi$ ground state for NiO^+ (CuO^+ was not treated in ref 13). Their assignment was based on the identity and the bonding capability of the ground state configuration of the bare metal ions and on the assumption that the ground state of MO^+ corresponds to the bonding of the ground state M^+ (d^n or s^1d^{n-1}) with the ground state O (^3P, s^2p^4). In this sense, our computations result in ground states for MO^+, in which M^+ participates in its respective s^1d^{n-1} configurations. For Fe^+, the s^1d^6

(12) Fiedler, A.; Hrušák, J.; Koch, W.; Schwarz, H. *Chem. Phys. Lett.* **1993**, *211*, 242.
(13) Carter, E. A.; Goddard, W. A., III *J. Phys. Chem.* **1988**, *92*, 2109.
(14) (a) Hippe, D.; Peyerimhoff, S. D. *Mol. Phys.* **1992**, *76*, 293. (b) Hrušák, J.; Koch, W.; Schwarz, H. *J. Chem. Phys.* In press.
(15) (a) Ziegler, T. *Chem. Rev.* **1991**, *91*, 651. Also see: (b) Broclawik, E.; Salahub, D. R. *J. Mol. Catal.* **1993**, *82*, 117.
(16) Andersson, K.; Malmquist, P.-Å.; Roos, B. O.; Sadlej, A. J.; Wolinski, K. *J. Phys. Chem.* **1990**, *94*, 5483.
(17) Schröder, D.; Fiedler, A.; Schwarz, J.; Schwarz, H. *Inorg. Chem.* In press.
(18) Vosko, S. J.; Wilk, L.; Nusair, M. *Can. J. Chem.* **1980**, *58*, 1200.
(19) Becke, A. D. *Phys. Rev.* **1988**, *A38*, 2398.
(20) Perdew, J. P. *Phys. Rev.* **1986**, *B33*, 8822 (Erratum *ibid.* **1986**, *B34*, 7406).
(21) The ADF package is available from: te Velde, G.; Baerends, E. J.; Department of Theoretical Chemistry, Vrije Universiteit, Amsterdam, The Netherlands.
(22) Schmidt, M. W.; Baldridge, K. K.; Boatz, G. A.; Jensen, J. H.; Koseki, S.; Gordon, M. S.; Nguyen, K. A.; Windus, T. L.; Elbert, S. T. *QCPE Bull.* **1990**, *10*, 52.
(23) Andzelm, J.; Wimmer, E.; Salahub, D. R.; Cray Res., Inc., 1991.
(24) Widmark, P.-O.; Malmqvist, P.-Å.; Roos, B. O. *Theor. Chim. Acta* **1990**, *77*, 291.
(25) Pou-Amerigo, R.; Merchan, M.; Widmark, P.-O. Manuscript in preparation.
(26) Andersson, K.; Fülscher, M. P.; Lindh, R.; Malmqvist, P.-Å.; Olsen, J.; Roos, B. O.; Sadlej; MOLCAS version 2, University of Lund, Sweden; Widmark, P. O.; IBM Sweden, 1992.

Table 1. Bond Lengths (in Å) and Excitation Energies ΔE (in eV) of the Low-Lying States of the Metal Oxide Cations MO^+ at the NLSD Level of Theory

	configuration[a]	$r(M^+-O)$	ΔE
FeO^+	$^6\Sigma^+$ $1\sigma^2 2\sigma^2 1\pi^4 1\delta^2 2\pi^2 3\sigma^1$	1.62	0.0
	$^4\Delta$ $1\sigma^2 2\sigma^2 1\pi^4 1\delta^3 2\pi^2 3\sigma^0$	1.56	1.0
	$^4\Phi$ $1\sigma^2 2\sigma^2 1\pi^4 1\delta^3 2\pi^1 3\sigma^1$	1.57	1.1
	$^4\Gamma$ $1\sigma^2 2\sigma^2 1\pi^4 1\delta^2 2\pi^2 3\sigma^1$	1.61	1.3
	$^4\Delta$ $1\sigma^2 2\sigma^2 1\pi^4 1\delta^2 2\pi^2 3\sigma^1$	1.63	1.4[b]
CoO^+	$^5\Delta$ $1\sigma^2 2\sigma^2 1\pi^4 1\delta^3 2\pi^2 3\sigma^1$	1.63	0.0
	$^3\Sigma^-$ $1\sigma^2 2\sigma^2 1\pi^4 1\delta^4 2\pi^2 3\sigma^0$	1.55	1.0
	$^3\Pi$ $1\sigma^2 2\sigma^2 1\pi^4 1\delta^4 2\pi^1 3\sigma^1$	1.55	1.2
	$^3\Delta$ $1\sigma^2 2\sigma^2 1\pi^4 1\delta^3 2\pi^2 3\sigma^1$	1.64	1.4[b]
NiO^+	$^4\Sigma^-$ $1\sigma^2 2\sigma^2 1\pi^4 1\delta^4 2\pi^2 3\sigma^1$	1.63	0.0
	$^4\Delta$ $1\sigma^2 2\sigma^2 1\pi^4 1\delta^3 2\pi^2 3\sigma^2$	1.74	1.1
	$^2\Delta$ $1\sigma^2 2\sigma^2 1\pi^4 1\delta^4 2\pi^2 3\sigma^1$	1.62	1.3[b]
	$^2\Pi$ $1\sigma^2 2\sigma^2 1\pi^4 1\delta^4 2\pi^1 3\sigma^2$	1.63	1.4
	$^2\Pi$ $1\sigma^2 2\sigma^2 1\pi^4 1\delta^4 2\pi^3 3\sigma^0$	1.63	1.6
	$^4\Phi$ $1\sigma^2 2\sigma^2 1\pi^4 1\delta^3 2\pi^3 3\sigma^1$	1.73	1.7
CuO^+	$^3\Sigma^-$ $1\sigma^2 2\sigma^2 1\pi^4 1\delta^4 2\pi^2 3\sigma^2$	1.76	0.0
	$^3\Pi$ $1\sigma^2 2\sigma^2 1\pi^4 1\delta^4 2\pi^3 3\sigma^1$	1.75	0.8
	$^1\Delta$ $1\sigma^2 2\sigma^2 1\pi^4 1\delta^4 2\pi^2 3\sigma^2$	1.73	1.4[b]
	$^1\Sigma^+$ $1\sigma^2 2\sigma^2 1\pi^4 1\delta^4 2\pi^4 3\sigma^0$	1.69	2.9

[a] The orbital labels follow from Figure 1. [b] State corresponding to the perfect pairing pattern; see text.

configuration is indeed the ground state. However, for Co^+, Ni^+, and Cu^+, the ground states correspond to s^0d^n configurations ($n = 8-10$). This appears to be the source of disparity between the present computational results and the qualitative assignment by Carter and Goddard.[13] Moreover, group VIII cations, as well as Cu^+, are known to utilize their s^1d^{n-1} configurations in bonding[2b,c] and to generate thereby significantly strong bonds, despite the large promotion energies for Ni^+ and Cu^+. We therefore conclude that our assignments of the ground states in Table 1 are reasonable. Nevertheless, following a more cautious approach, we have decided to focus attention on FeO^+, for which the ground and excited state assignments are solid.[12] Accordingly, we shall analyze the bonding features of FeO^+, the origins of its extremely low reactivity toward dihydrogen, and the other reactivity pattern shown in Scheme 1. Subsequently, we shall derive predictions regarding the reactivities of the other transition-metal oxide cations, on the basis of the electronic configurations of the ground and the first excited states of MO^+ (Table 1). As already shown by Carter and Goddard,[13] a blend of molecular orbital (MO) and valence bond (VB) arguments provides valuable insight into the bonding features of these species.

Figures 1 and 2 show the molecular orbital (MO) schemes and the contour maps for FeO^+ ($^6\Sigma^+$) as derived from the CAS calculations. According to the qualitative analysis of the wave functions these orbitals can be described as follows: (i) two doubly occupied σ-orbitals (1σ and 2σ, Figure 2, a and b) resulting from the interaction of the 2s and $2p_\sigma$ orbitals of oxygen with the s and d_σ orbitals of iron—the 1σ orbital largely originates from the 2s orbital of oxygen and thus hardly contributes to bonding, whereas the 2σ orbital gives rise to a strongly polarized σ bond; (ii) two degenerate and doubly occupied perpendicular π-orbitals (1π, Figure 2c), which represent the bonding combinations between the $2p_\pi$ orbitals of oxygen and the $3d_\pi$ orbitals of the iron; (iii) two singly occupied δ orbitals (1δ, Figure 2d), which do not find a symmetry match on oxygen and thereby remain pure nonbonding orbitals on iron; (iv) two perpendicular, degenerate singly occupied π orbitals (2π, Figure 2e), which correspond to the antibonding π^* orbitals of FeO^+; (v) a singly occupied mode of the d_σ orbital of iron (3σ, Figure 2f) with slightly antibonding character; and (vi) finally, the energetically demanding antibonding σ^* orbital (4σ, Figure 2g) corresponding to the lowest lying unoccupied MO which mainly exhibits the character of the 4s iron orbital. As

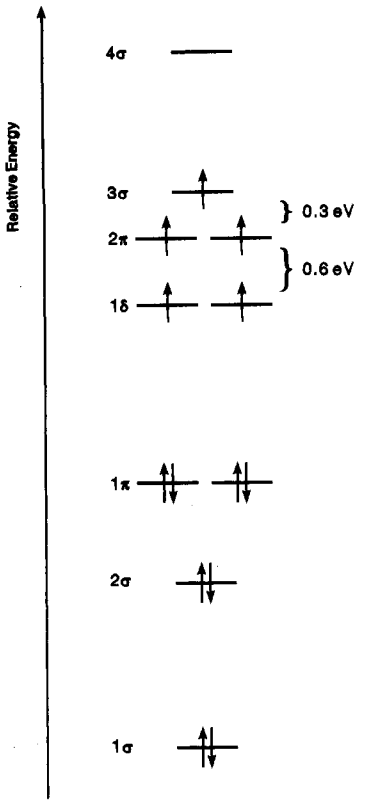

Figure 1. Qualitative molecular orbital scheme for FeO^+ ($^6\Sigma^+$). For the sake of clarity, the energy axis is not calibrated precisely.

indicated in Figure 1, the five singly occupied MOs (1δ, 2π, 3σ) are relatively close in energy; thus, according to Hund's rule the high-spin state $^6\Sigma^+$ is likely to be favored as the ground state of the FeO^+ molecule. More precisely, the energy gained by doubly occupying the lower-lying 1δ orbital in FeO^+ ($^4\Phi$) is overriden by the decreasing number of exchange energy terms as compared to the high-spin sextet state.[2b]

The comparison of the MO diagram for FeO^+ with the well-known electronic configuration of the triplet ground state of dioxygen reveals that both molecules exhibit a similar bonding situation; in particular, this comparison obviously accounts for the high-spin ground states of MO^+. The analogy of FeO^+ to O_2 has first been discussed by Carter and Goddard on the basis of a VB model.[13] In the VB description, the electronic structure in FeO^+ ($^6\Sigma^+$) may be subdivided into the nonbonding block which consists of $1\delta^2 3\sigma^1$ and the bonding block which consists of $2\sigma^2 1\pi_x^2 1\pi_y^2 2\pi_x^1 1\pi_y^1$. Focusing on the bonding block, FeO^+ ($^6\Sigma^+$) is seen to possess one σ bond and two π-type and mutually perpendicular 3-electron bonds ($1\pi_x^2 2\pi_x^1$ and $1\pi_y^2 2\pi_y^1$), in exact analogy to the bonding block in the $^3\Sigma_g^-$ ground state of O_2. By the same analogy we find a low-lying $^4\Delta$ excited state with a promotion energy of 1.4 eV, which possesses a double bond (σ and π) between Fe^+ and O and represents the perfect-pairing state analogous to $^1\Delta_g$ in singlet O_2. Of course, the perfect-pairing state of FeO^+ (Scheme 2b) suffers from 4-electron repulsion of the π electrons. To avoid this energetically demanding interaction, FeO^+ trades off perfect pairing for a more favorable configuration which consists of a σ bond and two resonating 3-electron π bonds in a high-spin situation (Scheme 2a). Furthermore, it is not surprising that the lowest excited states of FeO^+ do not correspond to the perfect pairing $^4\Delta$ state but rather to another $^4\Delta$ and a $^4\Phi$ state (Table 1), which arise from an electron excitation from the 3σ orbital or the 2π orbitals, respectively, to the 1δ manifold. Thus, the low-lying $^4\Delta$ state can be described by the same bonding mnemonic as depicted in Scheme 2a, and the $^4\Phi$ state involves a π bond in

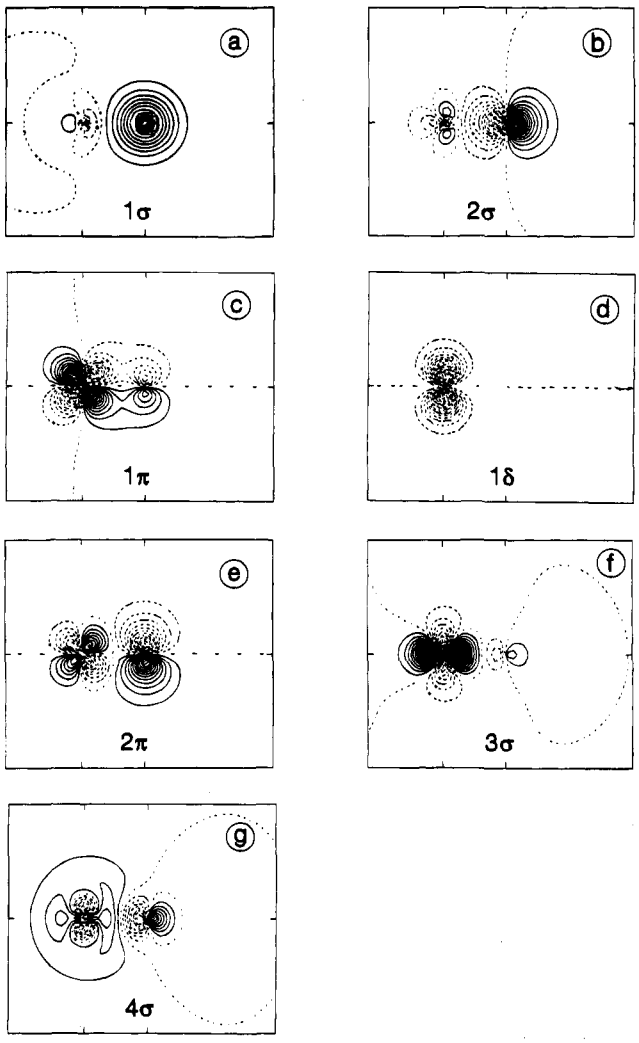

Figure 2. Contour diagrams of the atomic natural orbitals of FeO^+ ($^6\Sigma^+$) as derived from the CAS calculations.

Scheme 2

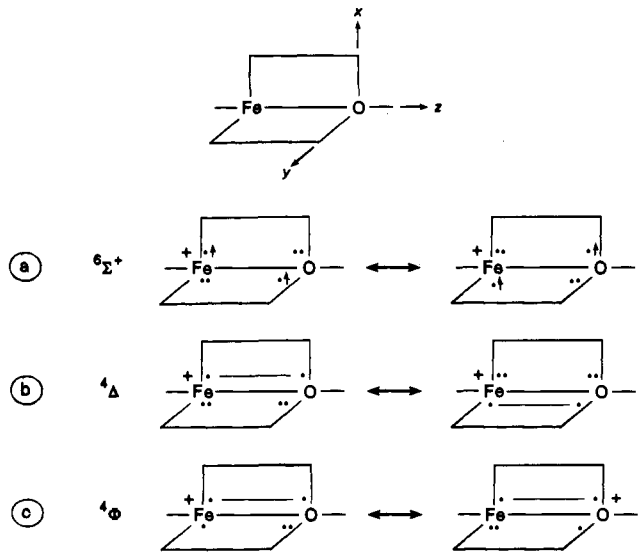

one plane[27a] and three weakly resonating π electrons in a perpendicular plane (Scheme 2c).[27b]

According to our calculations, the O_2 analogy is preserved also for the ground states of the other late-transition-metal oxide cations CoO^+, NiO^+, and CuO^+. Here, the additional electrons populate the nonbonding block and therefore do not affect the bonding situations which are still described in terms of Figure 1. Thus, in CoO^+ the additional electron populates a 1δ orbital, giving rise to the $^5\Delta$ state, in NiO^+ the 1δ orbitals continue to be populated and form a closed subshell of the $1\delta^4$ variety, resulting in a $^4\Sigma^-$ ground state, and in CuO^+ the extra electron populates the nonbonding 3σ orbital leading to a $^3\Sigma^-$ ground state. The generalized ground state VB mnemonic is shown in Scheme 3, and again the high-spin ground states can easily be rationalized by the analogy to dioxygen.

Scheme 3

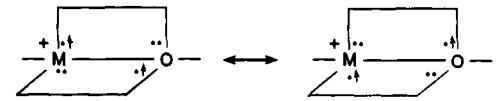

$^6\Sigma^+$ (Fe^+); $^5\Delta$ (Co^+); $^4\Sigma^-$ (Ni^+); $^3\Sigma^-$ (Cu^+).

The Carter–Goddard assignments for CoO^+ and NiO^+ differ from the present ones:[13] (i) For CoO^+ Carter and Goddard predict a $^3\Sigma^-$ ground state. As may be seen from the corresponding entry in Table 1, this state corresponds to the first excited state of CoO^+ and is generated from the $^5\Delta$ ground state by moving an electron from the 3σ to the 1δ orbital within the nonbonding block. Thus, both the $^5\Delta$ and the $^3\Sigma^-$ states possess the same bonding block which is represented by the VB mnemonic description in Scheme 3 and which follows the O_2 bonding paradigm. (ii) For NiO^+ Carter and Goddard predict a $^2\Pi$ ground state which is generated from the O_2-like $^4\Sigma^-$ state by moving an electron from 3σ to the π manifold.[13] Thus, NiO^+ ($^2\Pi$) has seven electrons in the π manifold and is therefore an O_2^- analogue with the π radical located more on the Ni center. According to Table 1 this excitation demands 1.6 eV and the erroneous assignment of Carter and Goddard originates from their assumption that the s^0d^9 ground state of Ni^+ forms the ground state metal oxide cation.

In summation, both FeO^+ and CoO^+ possess O_2-like bonding and are therefore perpendicular π-biradicals. According to the NLSD results, the situation for NiO^+ and CuO^+ is also O_2-like, but somewhat different from the qualitative assignment by Carter and Goddard. Since the bonding capability of the 4s orbitals is known to be better than that of the d_σ orbital,[2b,c] it is very likely that the assignment by Carter and Goddard, which did not consider explicitely this factor, is not valid.

Finally, as pointed out by a referee, it is noteworthy that the bond distances of the MO^+ ions correlate well with the number of electrons n^* in the formally antibonding 2π and 3σ orbitals: For $n^* = 2$ the distance amounts to 1.56 (±0.02) Å, for $n^* = 3$ the distance increases to 1.63 (±0.02) Å, and the distance reaches 1.74 (±0.02) Å for $n^* = 4$. The only state which deviates from this scheme is the highly-excited $^1\Sigma^+$ state of CuO^+ in which $r(M^+-O)$ amounts to only 1.69 Å, albeit both antibonding 2π orbitals are doubly occupied.

B. Reaction of FeO^+ with Dihydrogen. Consider the reaction of FeO^+ with molecular hydrogen (Figure 3) as a model for the reactivity of late-transition-metal oxide cations. The geometries of all relevant species which are nascent from the ground sextet state and the excited quartet states (Scheme 4) were optimized by using the NLSD approach, and the energetics were refined at the CASPT2D level of theory. With respect to the different symmetries of **1**, **2**, and **3** (Table 2), we restrict ourselves to a discussion of the energetically lowest-lying quartet and sextet states by appeal to Figure 3.

Initially, FeO^+ and dihydrogen approach each other to form a rovibrationally excited encounter complex, $(H_2)FeO^+$ (**1**). In the sextet surface, the energy-minimized geometry of $^6A'$-**1** can

(27) (a) There are two more equivalent structures with the π bond in the yz plane. (b) The right-hand-side cartoon involves a formal positive charge on oxygen and is therefore a minor contributor.

Scheme 4

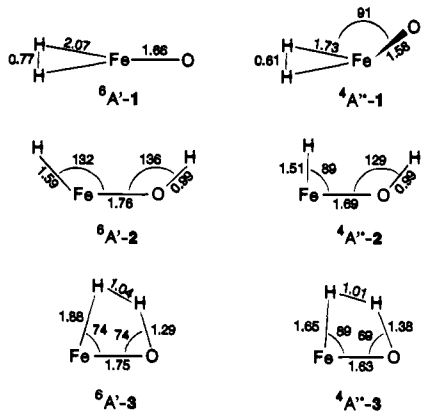

Table 2. Total Energies (hartrees) of Several Species Relevant for the Potential Energy Hypersurface for the Ion/Molecule Reaction of FeO^+ with Molecular Hydrogen[a]

	state	total energy
FeO^+	$^6\Sigma^+$	−1 338.096 02
FeO^+	$^4\Phi$	−1 338.065 53
H_2	$^1\Sigma_g^+$	−1.168 54
1	$^4A'$	−1 339.246 47
	$^4A''$	−1 339.258 69
	$^6A'$	−1 339.272 91
	$^6A''$	−1 339.203 74
2	$^4A'$	−1 339.300 19
	$^4A''$	−1 339.310 72
	$^6A'$	−1 339.287 64
	$^6A''$	−1 339.194 44
3	$^4A'$	−1 339.245 39
	$^4A''$	−1 339.255 51
	$^6A'$	−1 339.235 09
	$^6A''$	−1 339.189 02

[a] CASPT2D//NLSD level of theory.

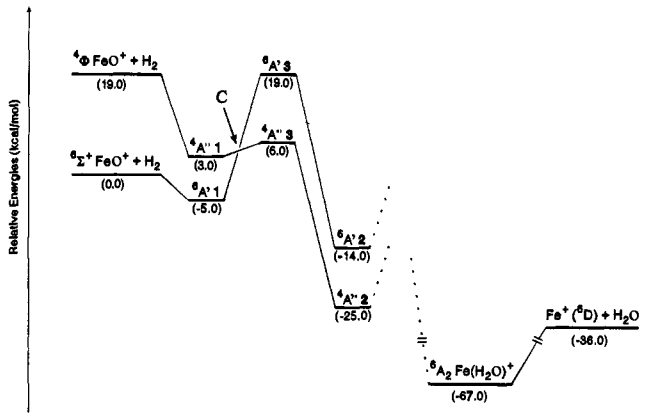

Figure 3. Potential energy surface for the reactions of FeO^+ ($^6\Sigma^+$) and FeO^+ ($^4\Phi$) with molecular hydrogen. (All energies in kcal/mol.) **C** denotes the location of the spin state crossover. The energetics of $Fe(H_2O)^+$ and $Fe^+ + H_2O$ were taken from ref 31. For the sake of clarity, TSs for the conversions of $^6A'$-**2** and $^4A''$-**2** to the final products are omitted; see text for details.

be described as a planar, C_{2v} symmetrical side-on complex of dihydrogen being attached to the iron. Due to the low polarizability of H_2, the fact that electron donation from the σ orbital of H_2 would involve the energetic 4σ orbital of FeO^+, and the repulsion between the σ orbital of H_2 and the singly-occupied 3σ orbital of FeO^+, the stabilization of $^6A'$-**1** with respect to the isolated ground state molecules amounts to only 5 kcal/mol. In contrast, in the corresponding quartet electromer $^4A''$-**1**, the analogous planar, C_{2v} symmetrical structure exhibits an imaginary frequency ($i209$ cm^{-1}) and corresponds to the transition state for a pseudorotation. The minimum structure of $^4A''$-**1** is not any more planar and exhibits C_s symmetry with H_2 being attached to the iron such that the H−Fe−H plane is perpendicular to the Fe−O bond. This geometry difference can easily be rationalized by the favorable orbital overlap of dihydrogen with FeO^+ in its quartet state: Here, the doubly occupied σ orbital of H_2 can interact with an energetically low-lying unoccupied orbital on iron and vice versa back-donation from a doubly occupied 1δ orbital at the Fe center to the empty σ^* orbital of H_2 can occur. This bonding situation is reflected in a significant elongation of the H−H bond to 0.81 Å in the quartet as compared to 0.77 Å in the sextet structure, as well as a substantial shortening of the Fe−H bond to 1.73 Å in $^4A''$-**1** as compared to 2.07 Å in $^6A'$-**1**. Thus, it is not surprising that the stabilization of $^4A''$-**1** with respect to isolated H_2 and FeO^+ ($^4\Phi$) amounts to 16 kcal/mol; this is much larger as compared to the sextet surface. Consequently, the multiplet splitting of 19 kcal/mol in isolated FeO^+ decreases to 8 kcal/mol by complexation of the dihydrogen molecule.

Let us now address the energetics of the primary products of the activation process, i.e., the inserted hydrido iron hydroxide cations,[28] H−Fe−OH^+ (**2**). Here, the difference in the stabilization energies of the $^4A''$ and $^6A'$ electromers is even more pronounced, so much so that the order of relative stabilities of sextet and quartet states is reversed with $^4A''$-**2** being the ground state. Whereas $^6A'$-**2** is only 14 kcal/mol energetically more stable as compared to the entrance channel of the isolated molecules, the $^4A''$-**2** quartet state experiences a much larger stabilization. Thus, $^4A''$-**2** is 11 kcal/mol more stable than its sextet electromer $^6A'$-**2**, it is located 25 kcal/mol below the sextet entrance channel, and it is stabilized by 44 kcal/mol with respect to isolated FeO^+ ($^4\Phi$) and dihydrogen. The energetics are reflected by the geometry differences between the $^4A''$ and the $^6A'$ electromers; for example, the bond lengths r(Fe−H) and r(Fe−O) are significantly smaller in the quartet ground state $^4A''$-**2** as compared to the sextet species $^6A'$-**2** (1.51 Å *versus* 1.59 Å and 1.69 Å *versus* 1.76 Å, respectively).[29] The difference between the electromers of the products is fundamental. Thus, $^4A''$-**2** involves two covalent bonds, O−H and Fe−H, whereas $^6A'$-**2** may be viewed as a weak coordination of H• to a quintet $FeOH^+$.[30] In fact, the same principle as before operates here too, since spin conservation in a sextet situation does not allow the formation of two new bonds between H_2 and FeO^+ ($^6\Sigma^+$). Any attempt to force the Fe−H interaction will result in populating an antibonding orbital, just so that total high spin is conserved. This is indeed born out from the calculations which reveal that the Fe−O bond in $^6A'$-**2** and $^6A'$-**3** is destabilized by population of the antibonding 4σ orbital. We note in passing that the methyl analog of **2**, CH_3−Fe−OH^+, was previously assigned to exhibit a sextet ground state.[6b] In view of the present results, we expect that CH_3−Fe−OH^+ will also have a quartet ground state, and the erroneous assignment was due to limitations of the theoretical approach used in the earlier study.

(28) Magnera, T. F.; David, D. E.; Michl, J. *J. Am. Chem. Soc.* **1989**, *111*, 4100.

(29) For both electromers the corresponding *trans* isomers are also minima on the potential energy surface; nonplanar structures were not localized as minima on the potential energy hypersurface. Since the NLSD energy differences of the *cis* and *trans* isomers are in the order of 1 kcal/mol and the *trans* isomers do not directly originate from the dihydrogen reaction, the energetics of these stereoisomers were not refined at the CASPT2D level.

(30) FeH^+, $FeOH^+$, $FeCH_3^+$, FeF^+, and $FeCl^+$ also exhibit quintet ground states, see for example: (a) References 2c and 6b. (b) Mandich, M. L.; Steigerwald, M. L.; Reents, W. D., Jr. *J. Am. Chem. Soc.* **1986**, *108*, 6197. (c) Langhoff, S. R.; Bauschlicher, C. W., Jr. *Annu. Rev. Chem.* **1988**, *39*, 181. (d) Schröder, D.; Hrušák, J.; Schwarz, H. *Helv. Chim. Acta* **1992**, *75*, 2215.

The $Fe(H_2O)^+$ complex,[31] which is probably generated as an intermediate in the sequence $FeO^+ \rightarrow \mathbf{1} \rightarrow \mathbf{3} \rightarrow \mathbf{2} \rightarrow Fe(H_2O)^+ \rightarrow Fe^+ + H_2O$, does not need to be analyzed in great detail in the present context. Based on the high stability of both $Fe(H_2O)^+$ and the separated products, i.e. Fe^+ and H_2O, the formation of $Fe(H_2O)^+$ from **2** is not likely to be associated with the rate-determining step of the reaction of FeO^+ with hydrogen, since the high exothermicities associated with their formation will lead to rapid dissociation into the products Fe^+ and H_2O. Furthermore, at the NLSD level of theory the TSs leading to formal 1,2-hydrogen migrations in **2** to yield $Fe(H_2O)^+$ are associated with activation barriers of 11 and 9 kcal/mol with respect to $^4A''$-**2** and $^6A'$-**2**. What remains, therefore, is to consider the primary activation process.

At the NLSD level of theory, transition structures (TS) **3** corresponding to the interconversion $\mathbf{1} \rightarrow \mathbf{3} \rightarrow \mathbf{2}$ could be localized for both the sextet and quartet multiplicities. The sextet TS $^6A'$-**3** is lying 19 kcal/mol above the FeO^+ ($^6\Sigma^+$) + H_2 ($^1\Sigma_g^+$) entrance channel, while the quartet TS $^4A''$-**3** is much lower in energy, being only 6 kcal/mol above the same entrance channel. This energetic difference is in line with the characteristic geometries of these two TSs (Scheme 4). Thus, all bonds in $^6A'$-**3** are substantially elongated as compared to the geometry of $^4A''$-**3**, indicating thereby a much higher degree of bond deformation in the sextet TS. This high degree of deformation in $^6A'$-**3** is also reflected in the high imaginary frequency (i1825 cm^{-1}) as compared to that of $^4A''$-**3** (i1476 cm^{-1}). Furthermore, both $^6A'$-**3** and its successor $^6A'$-**2** exhibit long Fe−H distances which suggest that these atoms are not strongly bonded and that the sextet pathway involves an asynchronous process of bond breaking and bond formation. The reasons for these features of the high-spin TS are precisely the reasons which led us to describe the primary high-spin product $^6A'$-**2** as a complex between H• and $FeOH^+$. Thus, the requirement to conserve the high spin results in a loss of bonding, and thereby to an energetically demanding TS as well as to an asynchronous mechanism. The requirement for spin conservation further imposes a very large barrier on the collapse of the biradicaloid product H•/$FeOH^+$ to **2**. This collapse is indeed forbidden by the Pauli exclusion principle (forcing triplet electrons into a bond). *Thus, the high-spin surface by itself is a dead end.* The quartet TS $^4A''$-**3** is fundamentally different. The geometry shows that it possesses intermediate bonding between its precursor ($^4A''$-**1**) and successor ($^4A''$-**2**) reactants and products, as if bond breaking and bond formation occur in concert. In fact, the quartet state reaction looks like an analog of a [2 + 2] cycloaddition reaction. This can be described by turning to the FeO^+ bonding mnemonics for $^4\Delta$ and $^4\Phi$ as depicted in Scheme 2. In organic chemistry such a cycloaddition is a formally forbidden process,[1a] which might have been considered to proceed via a high barrier and in a stepwise manner. However, formally forbidden processes may possess small barriers when the characteristic excitation energies for the cycloaddition are small and also when d orbitals are involved.[32] Similarly, the rather asymmetric nature of a $^4A''$-**3** may result in pericyclic bonding and in an effectively concerted process[32b,33] as revealed by the calculated potential energy surface. In summary, unlike the sextet surface, the quartet reaction can proceed smoothly to the insertion product. We conclude therefore that the only way to proceed from the sextet reactants to the quartet insertion product is by means of a crossover of both surfaces, as depicted in Figure 3. Thus, the overall reaction involves both spin-change and surmounting the barrier associated with $^4A''$-**3**.

The above scenario for the reaction of $FeO^+ + H_2$ with $^4A''$-**3** as the rate-determining transition structure accounts for the experimentally observed low rate constant for the ion/molecule reaction,[5] since it involves curve-crossing and a multicentered TS which act as an entropic bottleneck. As discussed previously[5] and seen now vividly from Figure 3, the reaction can proceed in a spin-conserving manner only by commencing with a formal $\mathbf{H^{\bullet}_T}$; however, this process is endothermic.

The *quantitative* aspects of the quartet surface are still unsatisfactory because $^4A''$-**3** is calcualted to be 6 kcal/mol *higher* in energy than the ground state entrance channel and, therefore, the reaction should not occur at all. Although the low efficiency of the process gave rise to speculation about the participation of ions steming from the high-energy tail of the thermal energy distribution,[5] we believe that the actual energy demand for the transition structure $^4A''$-**3** is lower than calculated. The reason for the energetic discrepancy between experimental and theoretical results is largely due to the still incomplete description of the energetics at the theoretical level: (i) As we have shown previously,[17] re-optimization of geometries obtained with the NLSD approach at the CASPT2D level of theory will slightly increase the stabilization energies. (ii) Further stabilization might be achieved by extension of the basis set on all four atoms.[12,17] (iii) In extensive *ab initio* calculations of the FeO^+ molecule,[12] we have shown that the CASPT2D approach overestimates the state splitting betwen $^6\Sigma^+$ and $^4\Phi$ states of FeO^+ as compared to QCISD(T) calculations. (iv) Finally, our computational approach neglects relativistic effects which may affect the relative stabilities. All these factors may be particularly relevant for the TS associated with the reaction $\mathbf{1} \rightarrow \mathbf{2}$. Another possibility for the discrepancy of experimental and theoretical findings is that we may have missed the energetically lowest-lying TS for the reaction of FeO^+ with H_2. However, all computational attempts to locate other four-centered TSs, e.g. nonplanar structures, lead to **3** or the stationary points described above. An alternative mechanism would involve a TS for a direct reaction of H_2 with the oxygen terminus of FeO^+; however, the oxygen atom in FeO^+ does not exhibit appropriate low-lying empty orbitals to react with H_2 in a concerted fashion and, thus, this pathway is expected to have a rather high energy demand. On the other hand, insertion of the Fe terminus into the H−H bond would lead to the high-energy isomer $(H)_2FeO^+$. At the NLSD level of theory this isomer is calculated to be 59 kcal/mol higher in energy than $^6A'$-**1**. Therefore, insertion at the Fe terminus was not further considered as a viable reaction path. Finally, the system might pass the energetic barrier associated with $^4A''$-**3** via quantum mechanical tunneling. However, a first-order Wigner correction[34] indicates that quantum mechanical tunneling is moderate and will not give rise to striking phenomena; this was also borne out in the experiments[5] in which no significant kinetic isotope effect for the reactions of H_2, HD, and D_2 was observed.

In spite of the discrepancies, the theoretical results provide a

(31) (a) Rosi, M.; Bauschlicher, C. W. B., Jr. *J. Chem. Phys.* **1989**, *90*, 7264. (b) Fiedler, A.; Hrušák, J.; Schwarz, H. *Z. Phys. Chem.* **1992**, *175*, 15.

(32) (a) Shaik, S. S.; Hiberty, P. C.; Ohanessian, G.; Lefour, J. M. *J. Phys. Chem.* **1988**, *92*, 5086. Here, it is shown how lowering the triplet energies stabilize transition state analogs of a [2 + 2] cycloaddition. (b) Seidl, E. T.; Grev, R. S.; Schaefer, H. F., III *J. Am. Chem. Soc.* **1992**, *114*, 3643. (c) For the role of transition metals in cycloadditions, see: Steigerwald, M. L.; Goddard, W. A., III *J. Am. Chem. Soc.* **1984**, *106*, 308.

(33) The interaction of the $^4\Delta$ state of FeO^+ with H_2 has two components. If we consider a certain plane of approach then in one resonance structure $^4\Delta$ has a π bond and in the other resonance structure $^4\Delta$ has four electrons. The former resonance structure resembles the [2 + 2] cycloaddition, while the latter can participate as a nucleophile attacking H_2. Similarly, $^4\Phi$ has a [2 + 2] and a radical attack component. The additional interactions weaken the orbital symmetry restrictions of the [2 + 2] cycloaddition.

(34) Bell, R. P. *The Tunnel Effect in Chemistry*; Chapman and Hall: London, 1980; pp 51.

possible scenario for the ion/molecule reaction of FeO^+ with dihydrogen, and the key results are as follows (Figure 3): Initially, the ground state FeO^+ ($^6\Sigma$) and H_2 form a rovibrationally excited encounter complex $^6A'$-**1** which undergoes a spin−orbit coupling mediated curve crossing from the sextet to the quartet hypersurface. Subsequently, $^4A''$-**1** reacts via the transition structure $^4A''$-**3** to form the inserted hydrido iron hydroxide cation $^4A''$-**2**. The so-formed intermediate **2** contains ca. 1 eV excess energy and rapidly decomposes either directly via reductive elimination or proceeding first to $Fe(H_2O)^+$, from which the final products Fe^+ and water are formed with an overall reaction exothermicity of 36 kcal/mol. With respect to the reaction kinetics, the low efficiency of the process can be rationalized by both the curve-crossing from the sextet to the quartet surface and the entropic restrictions associated with the multicentered transition structure $^4A''$-**3**, for which we estimate $\Delta S^{\ddagger}$ of −11 cal K^{-1} mol^{-1}. According to this model and in view of the importance of spin conservation arguments,[35] it can be expected that instead of the ^6D ground state the first excited ^4F electronic state of Fe^+ is formed as the ionic product. However, in the experimental setup used[5] it is practically impossible to examine the state of the cationic iron formed in the reaction of FeO^+ with dihydrogen, since the rate for the quenching process $Fe^+(^4F) \rightarrow Fe^+(^6D)$ exceeds that of its formation.[36] Consequently, any Fe^+ being isolated after a certain reaction period will exhibit ground state properties in its subsequent ion/molecule reactions. Other means will be required to probe the presence of the nascent $Fe^+(^4F)$ formed in the reaction of FeO^+ with H_2.

At this point we want to mention briefly an alternative, straightforward explanation for the low reactivity of FeO^+ toward dihydrogen, which, however, will not be pursued in detail furthermore. Although the $\mathbf{H^{\bullet}_T}$ process to generate separated $H^{\bullet}$ and $FeOH^+$ is endothermic[11,37] for H_2 and FeO^+ and does indeed not occur at thermal energies, the endothermicity is too small to exclude *a priori* a predissociative $\mathbf{H^{\bullet}_T}$ mechanism. This would lead to the formation of a loosely bound complex of $FeOH^+$ with a hydrogen radical which may undergo a predissociative confluence with the product channel, i.e., a reaction of $H^{\bullet}$ with $FeOH^+$, in which Fe^+ and water are formed as the final products. Due to our inability to measure *intrinsic* kinetic isotope effects in the system $FeO^+ + X_2 \rightarrow Fe^+ + X_2O$ (X = H, D) and to determine the precise temperature dependencies, strictly speaking we cannot distinguish between the variant of a $\mathbf{H^{\bullet}_T}$ predissociative mechanism and the scenario depicted in Figure 3.

C. Qualitative Trends in the Reactivity of MO^+ Species. Having described in great detail the reaction of FeO^+ with H_2, we now attempt to draw some generalities on the reactivity patterns of the other late-transition-metal oxide cations. Our analysis is based on the NLSD assignment of the ground states as the high-spin species with an O_2-type bonding.

From the FeO^+ discussion it is apparent that the high-spin potential energy surface can lead only to stepwise mechanisms like $\mathbf{H^{\bullet}_T}$ or **ET**, because of the principle of spin conservation and the bonding constraints imposed to it. Thus, whenever $\mathbf{H^{\bullet}_T}$ or **ET** are endothermic with respect to the entrance channels, the high-spin channel will be turned off. On the other hand, the low-spin surfaces can also lead to multibond reactions (**A** or **AE**), be they concerted or stepwise,[32] and to other low-spin processes like $\mathbf{H^-_T}$. However, since the ground states of the metal oxide cations are high spin, most of the more complex processes require a crossover between both surfaces. As a consequence, the efficiency of the overall reactions will be largely dependent on the stabilities and lifetimes of the rovibrationally excited encounter complexes between MO^+ and the substrates.

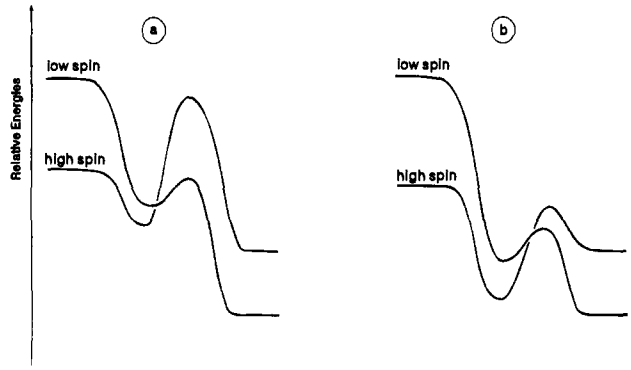

Figure 4. Qualitative potential energy surfaces for the reaction of ground state (high spin) and excited state (low spin) late-transition-metal oxide cations with organic substrates RH having small (a) and large (b) stabilization energies for the $MO(RH)^+$ encounter complexes.

Figure 4 shows the role of the stability of the encounter complexes. A situation as depicted in Figure 4a holds true for the reaction of MO^+ (M = Fe, Co, Ni) with H_2, where the stabilization energy is small. In these cases, the reaction which originates from the high-spin surfaces must surmount a significant barrier in addition to the spin-inversion requirement. Thus, it is not surprising that the rate constants k_R for the reactions of FeO^+, CoO^+, and NiO^+ with dihydrogen are much smaller than the collisional limits k_C, although the thermochemical driving forces ΔH_R to yield the metal cations and water are quite large (k_R/k_C = 0.01, 0.001, and 0.002; ΔH_R = −36, −41, and −54 kcal/mol for Fe, Co, and Ni, respectively).[5,39] No reactivity data exist for CuO^+, but it is obvious that for the high-spin $^3\Sigma^-$ ground state the efficiency of the reaction $CuO^+ + H_2 \rightarrow Cu^+ + H_2O$ will also be low. Quite a different situation is obtained for larger stabilization energies (Figure 4b). Here, the barrier will be substantially lower on the low-spin surface than the high-spin entrance channel, and the reaction will then only face an intersystem crossing bottleneck and thus may proceed with higher efficiency. Moreover, large stabilization energies are also likely to cause lower barriers on the high-spin surface and thereby to turn on the $\mathbf{H^{\bullet}_T}$ and **ET** mechanisms and stepwise activation processes.

The experimental data available are in accord with this analysis. For example, in the reaction of FeO^+ with methane, $\mathbf{H^{\bullet}_T}$ to yield $FeOH^+$ and $CH_3^{\bullet}$ (57% of all reaction products; k_R/k_C = 0.2) is thermochemically allowed and occurs relatively fast.[6a,38] In spite of this, methanol formation, presumably via an **I** mechanism involving the low-spin surface, can still compete with the hydrogen abstraction process (41%).[6a] As the latter reaction is thermochemically allowed for the quartet and the sextet surfaces, it may serve as an example belonging to the category depicted in Figure 4b, in which the high-spin and the low-spin channel can occur simultaneously. In addition, recent

(35) For numerous examples of state-selective chemistry and further references, see: (a) Armentrout, P. B. *Annu. Rev. Phys. Chem.* **1990**, *41*, 313. (b) Armentrout, P. B. *Science* **1991**, *251*, 175.

(36) Elkind, J. L.; Armentrout, P. B. *J. Phys. Chem.* **1986**, *90*, 5736.

(37) Throughout this article for the heat of formation of $FeOH^+$ we refer to the value given in ref 11. However, yet unpublished results indicate that $\Delta H_f(FeOH^+)$ is somewhat lower than the value given in ref 11, and according to these results the reaction $FeO^+ + H_2 \rightarrow FeOH^+ + H^{\bullet}$ is exothermic by 5 kcal/mol, see: Chen, Y.-M.; Clemmer, D. E.; Armentrout, P. B. Manuscript in preparation.

(38) Recently, the reactions of FeO^+ with H_2 and CH_4 have been studied by a complementary mass spectrometric technique and essentially the same results were obtained. For details, see: Clemmer, D. E.; Chen, Y.-M.; Khan, F. A.; Armentrout, P. B. *J. Phys. Chem.* **1994**, *98*, 6522.

(39) (a) Ryan, M. F.; Fiedler, A.; Schröder, D.; Schwarz, H. *Organometallics*. In press. (b) Chen, Y.-M.; Clemmer, D. E.; Armentrout, P. B. *J. Am. Chem. Soc.* **1994**, *116*, 2815.

Scheme 5

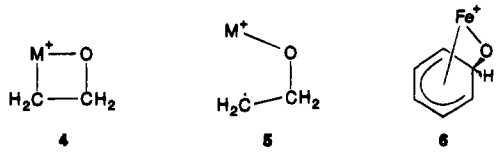

studies by Armentrout and co-workers indicate that the $FeOH^+$ formation also occurs via an insertion mechanism.[38] Similarly, NiO^+ reacts quite efficiently ($k_R/k_C = 0.2$),[40] whereas CoO^+ is much less reactive towards methane ($k_R/k_C = 0.002$).[39] As found for the activation of H_2, the low efficiency of methanol formation from methane, when reacted with CoO^+, indicates that the **I** mechanism involving excited MO^+ species is less favored for cobalt. When the polarizabilities and the density of states are increased by passing from methane to higher alkanes (RH), the complexation energies and the lifetimes of the encounter complexes $MO(RH)^+$ are increased too; furthermore, new reaction channels may open up, e.g. β-hydrogen transfer, having much lower activation barriers and thus resulting in a more facile oxidation of the higher alkane homologues. Indeed, the reaction rates of FeO^+, CoO^+, and NiO^+ with higher alkanes approach the collision limit.[7,39a,40]

The scenario outlined above can also be used to provide a better understanding of the reactions of unsaturated hydrocarbons with metal oxide cations, for which metallaoxetanes (e.g. **4**) are proposed as central intermediates (Scheme 5).[41] According to the analysis in terms of the O_2-type analogy, these metallacycles are nascent from the excited surface of the metal oxide cations and the high efficiencies of these processes[8,39a,40] can be attributed to the much larger complexation energies of alkenes as compared to that of alkanes.[42] The increasing complexation energies will also render the stepwise, spin-allowed reaction on the high-spin surface energetically feasible. This will lead to the corresponding high-spin metallacycles, and their radicaloid character, as indicated by **5**, and explains the subsequent isomerization to the corresponding carbonyl compounds, as is observed experimentally, e.g. $FeO^+ + C_2H_4 \rightarrow CH_3CHO$.[8b,c] We note in passing that very similar transformations of olefins have been observed in the corresponding reactions with O_2 ($^3\Sigma^-$).[45] Similarly, in the reaction of FeO^+ with benzene to yield phenol/Fe^+ and its subsequent decomposition products,[9] $\mathbf{H^{\bullet}_T}$ as well as **ET** are endothermic. Consequently, the reaction may either involve an **AE** mechanism, which is nascent from a quartet state, or the formation of a C–O bond in a σ-type complex **6**, being derived from the sextet surface and thus product formation is observed with high efficiency. In the ion/molecule reaction of FeO^+ with toluene the dominant reaction pathway leads to the formation of *neutral* FeOH and $C_6H_5CH_2^+$.[10] Here, the weak benzylic CH bond renders $\mathbf{H^{\bullet}_T}$ quite exothermic, but nevertheless this is *not* observed as such. In addition, thermoneutral **ET** to yield $C_7H_8^{\bullet+}$ cannot compete with the oxidation process. Although in this case one might involve either **AE** mechanism or $\mathbf{H^-_T}$ via the excited surface, it is equally attractive to consider a combination of a rapid primary $\mathbf{H^{\bullet}_T}$ and subsequent **ET** (or the reverse sequence), such that an initial $\mathbf{H^{\bullet}_T}$ leads to the formation of a benzyl radical which subsequently undergoes in the loosely interacting $C_6H_5CH_2^{\bullet}/FeOH^+$ complex a rapid charge transfer and spin inversion[46] to yield neutral FeOH and the benzyl cation $C_6H_5CH_2^+$.

Conclusions

The O_2 bonding analogy for the cationic late-transition-metal oxides appears to be a very useful paradigm for understanding and describing the bonding situation in MO^+ (M = Fe, Co, Ni, and Cu). The analogy also allows the classification of various experimentally observed reaction channels of MO^+ with hydrocarbon molecules.

The high-spin ground states of MO^+ exhibit a biradicaloid bonding and their reactivity is limited to atom abstraction and electron transfer processes. On the other hand, the excited low-spin electromers can also participate in multibond reactions such as cycloadditions or anion transfers. The communication between both spin surfaces is mediated by spin–orbit coupling induced spin flips.[46,47] This analogy is illustrated in detail for the reaction of FeO^+ with H_2, for which our quantum mechanical calculations follow the scenario outlined above: The reaction occurs via a multicentered transition structure and involves a crossover from the sextet surface entrance channel to the products which stem from the quartet surface. The reaction is completed by elimination of water which might eventually involve another spin flip to generate the sextet ground state $Fe^+(^6D)$. Application of these criteria to reactions of MO^+ with other organic substrates serves for the rationalization of the experimentally observed reaction kinetics and product distributions. In general, the analysis of the bonding in MO^+ in terms of molecular orbital and valence bond theory allows the prediction of state-selective reactivities, and once these concepts are established, a bridge forms between transition-metal and organic chemistry.

Acknowledgment. This research was supported by the Deutsche Forschungsgemeinschaft, the Fonds der Chemischen Industrie, and the Basic Research Foundation administered by the Israelian National Academy of Sciences and Humanties. H.S. is grateful to the Alexander von Humboldt-Foundation for a Max Planck Research-Award (jointly with Chava Lifshitz, The Hebrew University of Jerusalem). We thank Prof. P. O. Widmark for providing us with the ANO basis set for iron and Prof. P. Armentrout for communicating his results on FeO^+ and CoO^+ prior to publication.[38,39b] We are indebted to Ph.D. M. R. Ryan, Dr. H. Zipse, and the referees for helpful comments.

(40) Ryan, M. F.; Schwarz, H. Unpublished results.
(41) Jørgensen, K. A. *Chem. Rev.* **1989**, *89*, 431.
(42) Precise bond dissociation energies for FeO^+ and organic ligands are not known. However, it is reasonable to expect similar magnitudes as for the bare metal cation, for which the BDE(C_2H_4/Fe^+) of 34 kcal/mol (ref 43) largely exceeds that of the corresponding alkane; BDE(C_2H_6–Fe^+) = 15 kcal/mol (ref 44).
(43) Freiser, B. S. *Chemtracts—Anal. Phys. Chem.* **1989**, *1*, 65.
(44) Schultz, R. H.; Armentrout, P. B. *J. Phys. Chem.* **1992**, *96*, 1662.
(45) (a) Demole, E. *Chem. Ber.* **1878**, *11*, 315. (b) Pericas, M. A.; Serratosa, F. *Tetrahedron Lett.* **1978**, 4969.
(46) For the analyses of molecular motions required in spin inversion, see: (a) Shaik, S. S. *J. Am. Chem. Soc.* **1979**, *101*, 2736. (b) Shaik, S. S. *J. Am. Chem. Soc.* **1979**, *101*, 3184. (c) Shaik, S. S.; Epiotis, N. D. *J. Am. Chem. Soc.* **1980**, *102*, 122. (d) Larson, J. R.; Epiotis, N. D.; McMurchie, L. E.; Shaik, S. S. *J. Org. Chem.* **1980**, *45*, 1388.
(47) For recent studies of spin–orbit coupling in transition-metal compounds and further references, see: (a) Mitchell, S. A. In *Gas Phase Metal Reactions*; Fontijn, A., Ed.; Elsevier: Amsterdam, 1992; pp 227. (b) Siegbahn, P. E. M.; Blomberg, M. R. A. *Organometallics* **1994**, *13*, 354.